

## RESEARCH ARTICLE

# Rapid cold hardening increases axonal Na<sup>+</sup>/K<sup>+</sup>-ATPase activity and enhances performance of a visual motion detection circuit in *Locusta migratoria*

R. Meldrum Robertson\* and Christopher D. Moyes

## ABSTRACT

Rapid cold hardening (RCH) is a type of phenotypic plasticity that delays the occurrence of chill coma in insects. Chill coma is mediated by a spreading depolarization of neurons and glia in the CNS, triggered by a failure of ion homeostasis. We used biochemical and electrophysiological approaches in the locust, *Locusta migratoria*, to test the hypothesis that the protection afforded by RCH is mediated by activation of the Na<sup>+</sup>/K<sup>+</sup>-ATPase (NKA) in neural tissue. RCH did not affect NKA activity measured in a biochemical assay of homogenized thoracic ganglia. However, RCH hyperpolarized the axon of a visual interneuron (DCMD) and increased the amplitude of an activity-dependent hyperpolarization (ADH) shown previously to be blocked by ouabain. RCH also improved performance of the visual circuitry presynaptic to DCMD to minimize habituation and increase excitability. We conclude that RCH enhances *in situ* NKA activity in the nervous system but also affects other neuronal properties that promote visual processing in locusts.

**KEY WORDS:** Insect, Locust, RCH, DCMD, Octopamine, Na<sup>+</sup>/K<sup>+</sup>-ATPase

## INTRODUCTION

Rapid cold hardening (RCH) in insects describes a rapid, phenotypic plasticity that provides protection against abiotic environmental stress (Teets and Denlinger, 2013). Originally described as increasing survival under exposure to normally lethal cold temperatures (Lee et al., 1987), RCH has since been shown to mitigate the effects of other stressors such as hypoxia (Gantz et al., 2020; Srithiphaphirom and Robertson, 2022; Teets et al., 2020). The sensitivity of insects to environmental chilling can be characterized by measuring the critical thermal minimum for normal behaviour (CT<sub>min</sub>), the temperature for chill coma onset (CCO) and the chill coma recovery time (CCRT) (Andersen et al., 2015; Hazell and Bale, 2011; Overgaard and MacMillan, 2017). RCH reduces both CT<sub>min</sub>, enabling behaviour at lower environmental temperatures, and CCRT, speeding recovery from chill coma (Findsen et al., 2013; Kelty and Lee, 1999; Srithiphaphirom et al., 2019; Teets et al., 2020), but the mechanisms underlying this neuromuscular resilience are unknown.

It has been established that shutdown of the insect CNS at extremes of temperature is associated with a spreading depolarization (SD) of neurons and glia (Andersen et al., 2018;

Andersen and Overgaard, 2019; Jørgensen et al., 2020; Robertson, 2004; Robertson et al., 2017; Rodgers et al., 2007, 2010). SD, which has been well characterized in mammals and insects, represents an abrupt failure of ion homeostasis within the CNS, and a collapse of ion gradients across neural membranes (for reviews, see Robertson et al., 2020; Rodgers et al., 2010; Spong et al., 2016)). Treatments that delay the onset of SD are thus likely to be effective by enhancing mechanisms of ion homeostasis such as the Na<sup>+</sup>/K<sup>+</sup>-ATPase (NKA). Indeed, the protection afforded by RCH is seen in an improvement in the recovery of ion homeostasis in the brain of *Drosophila melanogaster* (Armstrong et al., 2012) and in the haemolymph of *Locusta migratoria* (Findsen et al., 2013). Moreover, RCH delays the occurrence of ouabain-induced SD in *L. migratoria*, suggesting a role for NKA (Gantz et al., 2020). Cold acclimation is a slower process of phenotypic plasticity that is like RCH in its ability to enhance chill tolerance (Andersen et al., 2017; MacMillan et al., 2015a,b), although the mechanisms providing this protection may differ. Cold acclimation reduces NKA activity of *Drosophila* whole-body homogenates without altering temperature sensitivity or abundance of the NKA enzyme (MacMillan et al., 2015b). Similarly, in *Drosophila* head homogenates, cold acclimation that reduces CCO temperature and the temperature of SD onset also reduces NKA activity and the temperature sensitivity (Q<sub>10</sub>) of NKA activity (Cheslock et al., 2021). These results suggest that decreasing SD temperature is unexpectedly associated with reduced CNS NKA activity, which would be expected to impair ion homeostasis, and are interpreted as indicating that acclimation to reduce SD temperature in the brain is independent of NKA activity and may be mediated by alteration of other mechanisms that would impact ion homeostasis in the CNS (e.g. ion channels and/or septate junctions) (Cheslock et al., 2021). A problem with measuring NKA activity in tissue homogenates is that it cannot account for differential cellular distribution of NKA protein multimers, such as via trafficking from intracellular stores into the plasma membrane (Hou et al., 2014; Moyes et al., 2021). Short-term regulation of NKA can be achieved by controlling the abundance of NKA proteins located in the plasma membrane after post-translational maturation in the endoplasmic reticulum (Kryvenko et al., 2021). Additionally, the *in situ* activity can be influenced by mass action ratios (e.g. [ATP]/[ADP]×[P<sub>i</sub>]), or reversible regulators (both allosteric and covalent) and the lipids of the membrane environment (Moyes et al., 2021). Given the electrogenic nature of NKA, an alternative approach to assess NKA activity *in situ* in intact cells is to use electrophysiological techniques to directly measure the pump current (i.e. the ouabain-sensitive current) across cell membranes or, indirectly, the membrane hyperpolarization caused by the pump current (Moyes et al., 2021).

It is a common observation that a period of repetitive activity in nerve fibres is followed by a hyperpolarization whose amplitude is

Department of Biology, 3118 Biosciences Complex, Queen's University, Kingston, ON, Canada, K7L 3N6.

\*Author for correspondence (robertm@queensu.ca)

 R.M.R., 0000-0002-2666-7861

Received 3 February 2022; Accepted 28 April 2022

**List of abbreviations**

ADH	activity-dependent hyperpolarization
CCO	chill coma onset
CCRT	chill coma recovery time
CT <sub>min</sub>	critical thermal minimum
DA	depolarizing afterpotential
DCMD	descending contralateral movement detector
HA	hyperpolarizing afterpotential
LGMD	lobula giant movement detector
NKA	Na <sup>+</sup> /K <sup>+</sup> -ATPase
RCH	rapid cold hardening
SD	spreading depolarization

dependent on the duration and frequency of action potential firing. Since 1957, it has been known that this activity-dependent hyperpolarization (ADH) in mammalian non-myelinated axons is closely linked to the energy-dependent, ouabain-sensitive sodium pump (Ritchie and Straub, 1957). Subsequently, NKA-dependent ADH has been documented in, at least, blowfly photoreceptors (Gerster et al., 1997), *D. melanogaster* larvae (Pulver and Griffith, 2010), *L. migratoria* adults (Money et al., 2014), *Xenopus laevis* larvae (Zhang and Sillar, 2012) and neonatal mice (Picton et al., 2017a). Such dynamic NKA activity plays important roles in the control of motor patterning [e.g. *Drosophila* larval crawling (Pulver and Griffith, 2010); leech heartbeat (Kueh et al., 2016); *Xenopus* tadpole swimming (Hachoumi et al., 2022); neonatal mouse locomotion (Picton et al., 2017a)]. We chose to investigate the effect of RCH on an ADH recorded in the axon of the descending contralateral movement detector (DCMD) neuron of locusts because this is a large, accessible, identified neuron that fires in high-frequency bursts of large-amplitude action potentials.

The soma of the DCMD neuron is located in the brain and it extends a large-diameter axon to the metathoracic ganglion in the contralateral connective (Rowell, 1971). It is highly responsive to objects moving in the visual field ipsilateral to the soma, particularly looming stimuli, because of being driven to fire by the lobula giant movement detector (LGMD) interneuron (Gabbiani et al., 1999; Oshea et al., 1974; Rind, 1984; Rind and Simmons, 1992). The role of the DCMD is to relay bursts of high-frequency action potentials from the brain to motor centres in the thoracic ganglia, where it triggers escape and collision avoidance behaviours (Gray et al., 2001; Santer et al., 2006, 2005, 2008; Simmons et al., 2010). Axonal conduction in the DCMD shows phenotypic plasticity in response to heat shock (Money et al., 2005), anoxia (Money et al., 2014) and food deprivation (Cross et al., 2017). Notably, an ADH in response to electrical stimulation of the DCMD axon is blocked by ouabain, indicating that it is generated by the electrogenic NKA (Money et al., 2014). Given that information coding in the DCMD firing pattern is facilitated by firing bursts of action potentials at high frequencies (McMillan and Gray, 2015) and that high-frequency bursts are important for triggering escape behaviours (Santer et al., 2006), a useful way of characterizing performance of the DCMD axon is to monitor the ability to sustain high conduction velocities at high firing frequencies (Money et al., 2014). Supernormal conduction refers to the general axonal property, predicted from the Hodgkin–Huxley equations, whereby conduction velocity is increased for action potentials at 50–150 Hz relative to propagation of single action potentials as a result of a short period of supernormal excitability immediately following the relative

refractory period (Bucher and Goaillard, 2011; Hopf et al., 1976). Supernormal conduction has been described for the DCMD axon (Cross and Robertson, 2016) and is lost after recovery from an anoxic coma (Cross et al., 2017). Moreover, octopamine mediates the effects of RCH on chill coma (Srithiphaphirom et al., 2019) and on anoxic coma (Srithiphaphirom and Robertson, 2022) as well as stabilizing conduction reliability in the DCMD axon during hypoxia (Money et al., 2016). Thus, much prior research indicates that the DCMD axon generates an ADH at high frequencies of firing via activation of NKA and that this shows phenotypic plasticity in response to abiotic stress.

We used a biochemical approach to measure NKA activity of homogenized thoracic ganglia and an electrophysiological approach to evaluate NKA activity in the axon of the DCMD in control and RCH locusts. We found no effect of RCH on total NKA enzymatic activity measured spectrophotometrically in homogenates. However, RCH did enhance NKA activity measured electrophysiologically. We suggest that *in situ* NKA activity in the intact CNS contributes to the effects of RCH to delay coma, whether induced by chilling or anoxia, and to speed recovery.

**MATERIALS AND METHODS****Animals**

Adult locusts, *Locusta migratoria* (Linnaeus, 1758), were obtained from a crowded colony maintained in the Biosciences Complex at Queen's University. Room temperature in the colony was 25°C. During the light portion of a 12 h:12 h photoperiod (lights on at 07:00 h), incandescent light bulbs raised the temperature in the cages to ~30°C. The locusts were fed daily with a diet of wheat seedlings and a mixture of dried milk powder, yeast and wheat bran. Males and females at least 3 weeks past the imaginal moult were used for experiments.

**Rapid cold hardening**

Individual locusts were taken arbitrarily from the colony and held in ventilated plastic containers. RCH locusts were kept isolated in the dark at ~4°C for 4 h and allowed to recover for 1 h at room temperature (~22°C) before experiments (Srithiphaphirom et al., 2019). Control locusts were isolated in the dark at room temperature for 5 h.

**NKA assay**

We used 6 males and 6 females in each treatment for two replicate trials. Mesothoracic and metathoracic ganglia were collected from control and RCH locusts, frozen in liquid nitrogen and stored at –80°C. The NKA assay was based on Moyes et al. (2021). Subsequently, the ganglia were homogenized in 300 µl of lysis buffer (50 mmol l<sup>-1</sup> Hepes, 10 mmol l<sup>-1</sup> EDTA, 10 mmol l<sup>-1</sup> Chaps, pH 7.4) using a plastic pestle fitted to a microcentrifuge tube and ensuring that the tubes remained cold. The homogenate was centrifuged for 1.5 min at 10,000 rpm, and the supernatant removed and kept on ice. Assays were completed within 30 min of homogenization. The assay consisted of 50 mmol l<sup>-1</sup> Hepes (pH 7.4), 5 mmol l<sup>-1</sup> ATP, 20 mmol l<sup>-1</sup> NaCl, 20 mmol l<sup>-1</sup> KCl, 1 mmol l<sup>-1</sup> phosphoenolpyruvate, 5 mmol l<sup>-1</sup> MgCl<sub>2</sub>, 0.2 mmol l<sup>-1</sup> NADH, 4 U ml<sup>-1</sup> lactate dehydrogenase and 5 U ml<sup>-1</sup> pyruvate kinase. Each sample was added to 6 wells, 20 µl per well. Three wells included ouabain (final concentration, 0.5 mmol l<sup>-1</sup>). The assay was initiated with 250 µl of the complete assay mix. Reactions were run at 25°C for 7 min, and the absorbance decline at 340 nm was monitored for 7 min. The rates were determined from the initial linear decrease in absorbance. Protein measurements were made

using the Bio-Rad reagent, using bovine serum albumin as the standard. The activity was expressed per mg protein.

### Semi-intact preparation

We used a standard preparation of adult locusts for extracellular and intracellular recording of DCMD activity (Robertson and Pearson, 1982). After the wings and legs were cut off, locusts were pinned to a cork board and opened with a dorsal midline incision. Air sacs and fat body were removed, and the gut was cut posteriorly and reflected laterally out of the thorax. The mesothoracic and metathoracic ganglia were exposed and raised onto a stainless steel support. Nerves 3, 4 and 5 of both ganglia were cut to de-efferent thoracic muscles and minimize movement. The preparation was bathed in locust saline (in mmol l<sup>-1</sup>: 147 NaCl, 10 KCl, 4 CaCl<sub>2</sub>, 3 NaOH and 10 Hepes buffer; pH 7.2; chemicals from Sigma-Aldrich).

### Electrophysiology

The preparation was grounded with a chlorided silver wire placed in the open abdomen. We recorded DCMD activity extracellularly using a custom-made, glass suction electrode placed on the dorso-medial surface of the pro-meso connective about 1 mm anterior to the posterior edge of the mesothoracic ganglion. Electrical activity was filtered and amplified with a differential AC amplifier (A-M Systems Model 1700;  $\times 100$  amplification, low cut off at 300 Hz and

high cut off at 10 kHz). The same electrode was used to stimulate DCMD using an A-M Systems Isolated Pulse Stimulator (Model 2100).

Intracellular recordings were taken from the axon of DCMD as it exited the mesothoracic ganglion dorsally in the medial edge of the connective (Fig. 1A). We used borosilicate glass microelectrodes (WPI Inc.) pulled to a resistance of 20–40 M $\Omega$  when filled with 500 mmol l<sup>-1</sup> KCl. Signals were amplified  $\times 10$  using an A-M Systems Model 1600 Neuroprobe amplifier. The stray capacitance to ground through the wall of the electrode could severely attenuate the amplitude of DCMD action potentials by as much as 40 mV by acting as a low-pass filter. We adjusted the capacitance compensation circuitry by over-compensating to send the circuit into positive feedback and then backing off slightly to obtain the sharpest possible recording.

Signals were digitized using a 1440 A digitizer (Molecular Devices) and recorded using Axoscope 10.7 software. The sampling rate was maximized (250 kHz; interval 4  $\mu$ s) to ensure that the peak of the DCMD action potential was captured as faithfully as possible.

### DCMD stimulation

We used 16 control and 16 RCH locusts. Experiments were grouped so that 2 males and 2 females from the same cage in the colony (to

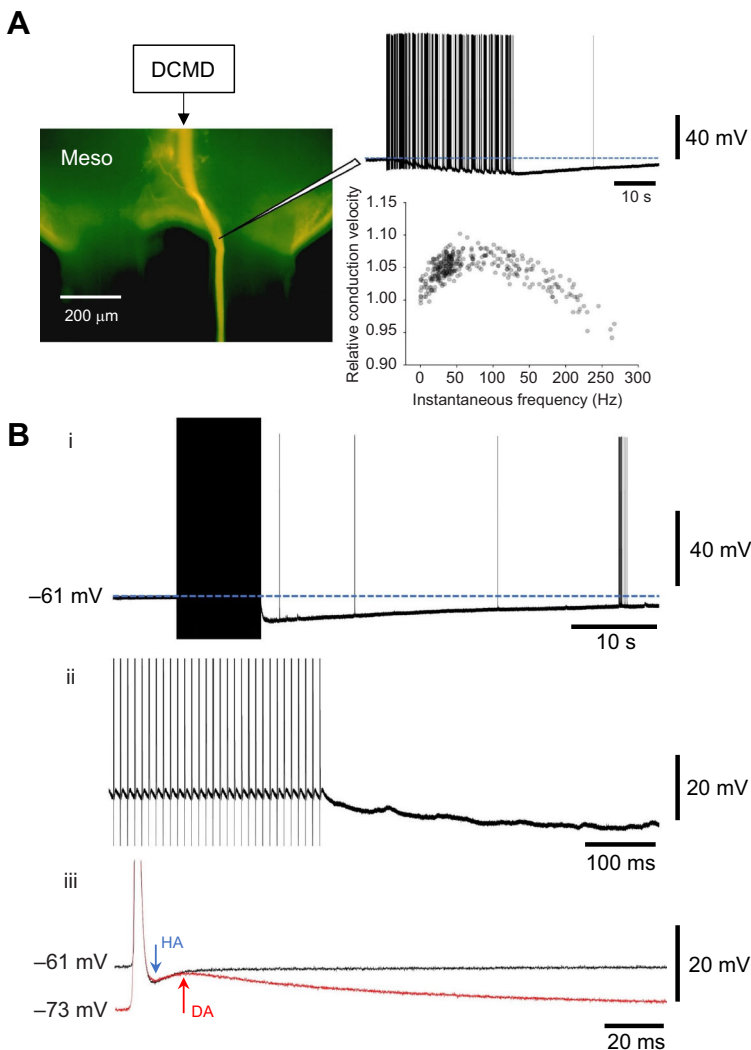


**Fig. 1. Characteristics of descending contralateral movement detector (DCMD) activity recorded intracellularly from the axon.** (A) Left: dorsal aspect of a Lucifer Yellow-filled DCMD axon (filled as described in Gray et al., 2010) exiting the mesothoracic ganglion (meso, anterior at top) in the meso-meta connective, illustrating the location of intracellular penetration for recording shown on the right. Right, top: visual stimulation generates a bursty pattern of high-frequency action potentials ( $\sim 100$  mV amplitude) and, after the end of visual stimulation, an activity-dependent hyperpolarization (ADH;  $\sim 15$  mV) lasting  $>30$  s. Membrane potential prior to stimulation was  $-60$  mV (blue dotted line). Right, bottom: for a different recording, supernormal axonal conduction is indicated by a 5–10% increase in conduction velocity for action potentials with instantaneous firing frequencies of 50–150 Hz compared with single action potentials (frequency  $\sim 0$  Hz). (Bi) Electrical stimulation of the axon in the pro-meso connective to generate a standard 10 s burst of 1000 action potentials at 100 Hz causes an ADH lasting  $>50$  s. Membrane potential prior to stimulation was  $-61$  mV (blue dotted line). (Bii) Expansion of the recording at the end of the burst. Note that the membrane potential is maintained during the burst and hyperpolarization occurs only after firing stops. (Biii) Overlay comparison of action potentials before (black trace) and after (red trace) stimulation. Note the 12 mV ADH revealing a depolarizing afterpotential (DA) in the red trace with a peak at 20 ms and lasting  $\sim 150$  ms. Also, the hyperpolarizing afterpotentials (HA) of the before and after action potentials overlap exactly, indicating that the delayed rectifier K<sup>+</sup> current is unaffected. The HA (blue downward arrow) is followed by the DA (red upward arrow), which sums during high-frequency activity to offset the ADH during DCMD bursts.



control for colony conditions) were examined on the same day and the order of experiments on different sexes was alternated on different days. For one of the RCH locusts, we were unsuccessful in penetrating DCMD intracellularly. Also, sample sizes decrease at higher firing frequencies ( $>500$  Hz) as individual preparations failed to reach the higher frequencies. We visually stimulated DCMD with hand movements in the visual field contralateral to the recorded axon (ipsilateral to the DCMD cell soma and dendrites) for at least 30 s. The procedure was to use swooping movements towards the eye in different portions of the visual field, thus minimizing habituation (Gray, 2005), to maximize the firing frequency and number of action potentials recorded (Fig. 1A). This method of stimulation is not instrumentally controlled but has the advantage of being more likely to maximally activate the visual circuitry and, by simulating predator attacks, is more natural than standard looming visual stimuli on a computer screen. For more control, we electrically stimulated the axon via the suction electrode to generate 1000 action potentials at 100 Hz for 10 s (Fig. 1B). Stimulus pulse duration was 4 ms and stimulus strength was adjusted to be the minimum required to generate action potentials throughout the train (stimulus efficacy reduced during the train as spike threshold gradually increased as a result of incomplete recovery from  $\text{Na}^+$  channel inactivation with successive action potentials at high frequency). This electrical stimulation protocol generates an ADH (Fig. 1Bi) that is eradicated after treatment with  $0.1 \text{ mmol l}^{-1}$  ouabain (Money et al., 2014).

### Data analysis

The firing pattern of DCMD generated by circuitry in the brain during visual stimulation was analysed by counting the number of spikes generated during 30 s of stimulation and characterizing the pattern of bursting. Burst firing is an important method of coding information dynamically for looming stimuli, where bursts have been defined as groups of spikes with interspike intervals  $\leq 8$  ms (i.e. firing frequency  $\geq 125$  Hz) (McMillan and Gray, 2015). In addition, DCMD firing frequencies  $>150$  Hz reliably trigger escape responses in flying locusts and six consecutive action potentials at 200 Hz trigger gliding if occurring at the correct phase of the flight cycle (Santer et al., 2006). Hence, we measured the number and duration of bursts  $\geq 125$  Hz (including frequencies  $>200$  Hz) and, separately,  $\geq 200$  Hz.

We measured the resting membrane potential of the DCMD axon, and the amplitude of the hyperpolarization generated by the controlled electrical stimulation. The amplitude of individual action potentials was measured from the positive peak to the negative peak of the hyperpolarizing afterpotential (HA). These values are unaffected by variation of the resting membrane potential caused by the changing NKA activity. The HA is followed by a depolarizing afterpotential (DA; Fig. 1Biii) that maintains excitability by counteracting the HA and promotes supernormal conduction (Cross and Robertson, 2016; Money et al., 2005). Action potential duration was measured at the half-amplitude. Conduction velocity in the axon was calculated from the latency between the extracellular and intracellular recordings ( $\sim 1$  mm apart). Relative conduction velocity was calculated relative to the conduction velocity at the highest interspike interval (lowest instantaneous firing frequency) for that individual.

Outliers in datasets were removed using Grubb's test online. Statistical comparisons were carried out using the software in Sigmaplot 14 (Systat Software Inc.). Data were tested for normality (Shapiro–Wilk test) and equal variance (Brown–Forsythe test) before applying parametric or non-parametric tests as appropriate.

When possible, data were transformed to fit the assumptions of parametric tests. In the Results, data are reported as means  $\pm$  s.d. or median (interquartile range, IQR).

## RESULTS

### NKA assay

RCH had no effect on the NKA activity of homogenized mesothoracic and metathoracic ganglia (Fig. 2). Comparison of the data from the two replicate assays (Table 1) by three-way ANOVA revealed no effect of trial ( $P=0.27$ ), no effect of sex ( $P=0.36$ ), no effect of treatment ( $P=0.90$ ) and no significant interactions ( $P_{\text{trial} \times \text{sex}}=0.19$ ;  $P_{\text{trial} \times \text{treatment}}=0.46$ ;  $P_{\text{sex} \times \text{treatment}}=0.88$ ;  $P_{\text{trial} \times \text{sex} \times \text{treatment}}=0.74$ ). There was also no effect of any factor on total ATPase activity of the samples (data not shown).

### DCMD firing pattern

RCH had no effect on the mean firing frequency in response to visual stimulation [control: 144 Hz (IQR 118–178 Hz); RCH: 138 Hz (IQR 113–163 Hz); Student's  $t$ -test on ln-transformed data  $P=0.84$ ] or on the peak frequency (control:  $763 \pm 146$  Hz; RCH:  $786 \pm 137$  Hz; Student's  $t$ -test  $P=0.66$ ). However, RCH did increase the total number of action potentials generated (control:  $359 \pm 134$ ; RCH:  $636 \pm 214$ ; Welch's  $t$ -test for unequal variances  $P=0.0002$ ) (Fig. 3A). RCH also increased the maximum duration of action potential bursts  $\geq 125$  Hz [control: 33.7 ms (IQR 25.4–50.7 ms); RCH: 55.6 ms (IQR 40.0–82.7 ms); Student's  $t$ -test on ln-transformed data  $P=0.04$ ] (Fig. 3B), but not the maximum duration of bursts  $\geq 200$  Hz [control: 13.6 ms (IQR 9.6–18.5 ms); RCH: 17.1 ms (IQR 14.0–25.7 ms); Student's  $t$ -test on ln-transformed data  $P=0.21$ ]. In addition, RCH increased the number of bursts  $\geq 125$  Hz (control:  $66.1 \pm 34.8$ ; RCH:  $106.8 \pm 44.6$ ; Student's  $t$ -test  $P=0.008$ ) (Fig. 3C) and the number of bursts  $\geq 200$  Hz (control:  $52.9 \pm 30.0$ ; RCH:  $95.3 \pm 48.6$ ; Student's  $t$ -test  $P=0.008$ ) (Fig. 3D).

### DCMD axonal action potential

RCH had no effect on the amplitude of DCMD action potentials recorded intracellularly in the axon (control:  $91.1 \pm 7.5$  mV; RCH:  $93.5 \pm 7.6$  mV; Student's  $t$ -test  $P=0.39$ ) (Fig. 4A) or on their duration

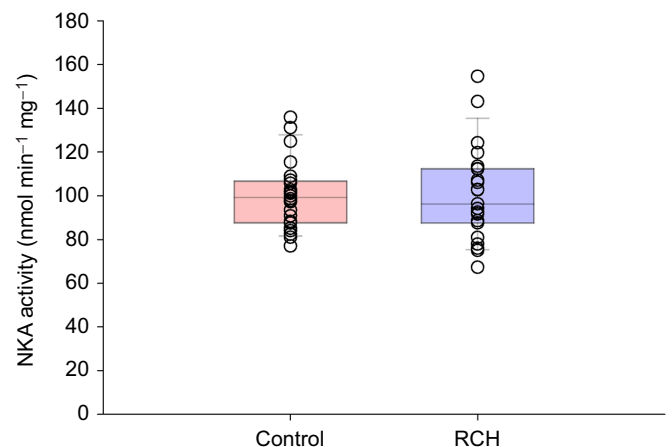


**Fig. 2. Rapid cold hardening (RCH) has no effect on  $\text{Na}^+/\text{K}^+$ -ATPase (NKA) activity of homogenized thoracic ganglia.** Data from 6 males and 6 females for each treatment in two replicates (see Table 1). Three-way ANOVA revealed no significant effects of sex, trial number or treatment and no interactions ( $P>0.05$ ). For illustration, the data for sex and trial number have been combined.

**Table 1. NKA activity in homogenized ganglia of control locusts and those subjected to rapid cold hardening (RCH)**

Group	NKA activity (nmol min <sup>-1</sup> mg <sup>-1</sup> )			
	Trial 1		Trial 2	
	Male	Female	Male	Female
Control	99.5±15.8 (n=6)	98.3±19.4 (n=6)	96.1±8.5 (n=6)	106.0±17.7 (n=6)
RCH	97.2±21.7 (n=6)	93.9±9.6 (n=6)	98.2±18.2 (n=5)	113.4±30.2 (n=6)

Data are means±s.d. One outlier (trial 2, male, RCH) was removed using Grubb's test on the complete dataset. Three-way ANOVA revealed no significant effects of trial number, sex or treatment and no significant interactions (see Results).

at half-amplitude (control: 0.28±0.06 ms; RCH 0.27±0.05 ms; Student's *t*-test *P*=0.48) (Fig. 4B). However, RCH hyperpolarized by 4.3 mV the resting membrane potential measured in the absence of any activity (control: -60.27±6.12 mV; RCH: -64.60±5.25 mV; Student's *t*-test *P*=0.047) (Fig. 4C) and increased by 1.5 mV the ADH induced by 30 s of visual stimulation (control: 2.7±1.4 mV; RCH: 4.2±1.9 mV; Student's *t*-test *P*=0.026; data not shown). For the visually stimulated ADH, there was no control over the number of action potentials or their frequency of firing. With controlled electrical stimulation, RCH increased by 2.37 mV the ADH induced by 10 s of action potential firing at 100 Hz (control: 4.5±2.99 mV; RCH: 6.87±2.50 mV; Student's *t*-test *P*=0.024) (Fig. 4D).

#### DCMD axonal conduction velocity

RCH had no effect on the maximum action potential conduction velocity recorded in the pro-mesothoracic connective, including traversing the mesothoracic ganglion (control: 3.46±0.62 m s<sup>-1</sup>; RCH: 3.63±0.67 m s<sup>-1</sup>; Student's *t*-test *P*=0.47) (Fig. 5A) or the minimum conduction velocity (control: 2.39±0.74 m s<sup>-1</sup>; RCH: 2.63±0.39 m s<sup>-1</sup>; Student's *t*-test *P*=0.30) (Fig. 5B). However,

RCH increased supernormal conduction in the axon at firing frequencies up to 500 Hz (Fig. 5C). RCH increased relative conduction velocity in different frequency ranges (two-way ANOVA: *P*<sub>treatment</sub><0.001; *P*<sub>frequency</sub><0.001; *P*<sub>treatment×frequency</sub>=0.97). In the 200–300 Hz frequency range, where relative conduction velocity peaked and supernormal conduction was maximal, RCH increased the relative conduction velocity by 7% (control: 1.01±0.088; RCH: 1.08±0.072; Student's *t*-test *P*=0.026).

#### DISCUSSION

We used two approaches to evaluate NKA activity in the nervous system of *L. migratoria* after RCH. A biochemical assay of NKA activity of homogenized thoracic ganglia showed no effect of RCH. However, intracellular recordings from the axon of the DCMD neuron showed that RCH hyperpolarized the resting membrane potential and increased the amplitude of the ADH generated by a standard electrical stimulation producing 1000 action potentials at 100 Hz for 10 s. Both effects are consistent with RCH enhancing the activity of NKA in the plasma membrane of the DCMD axon. In addition, we found that RCH increased the

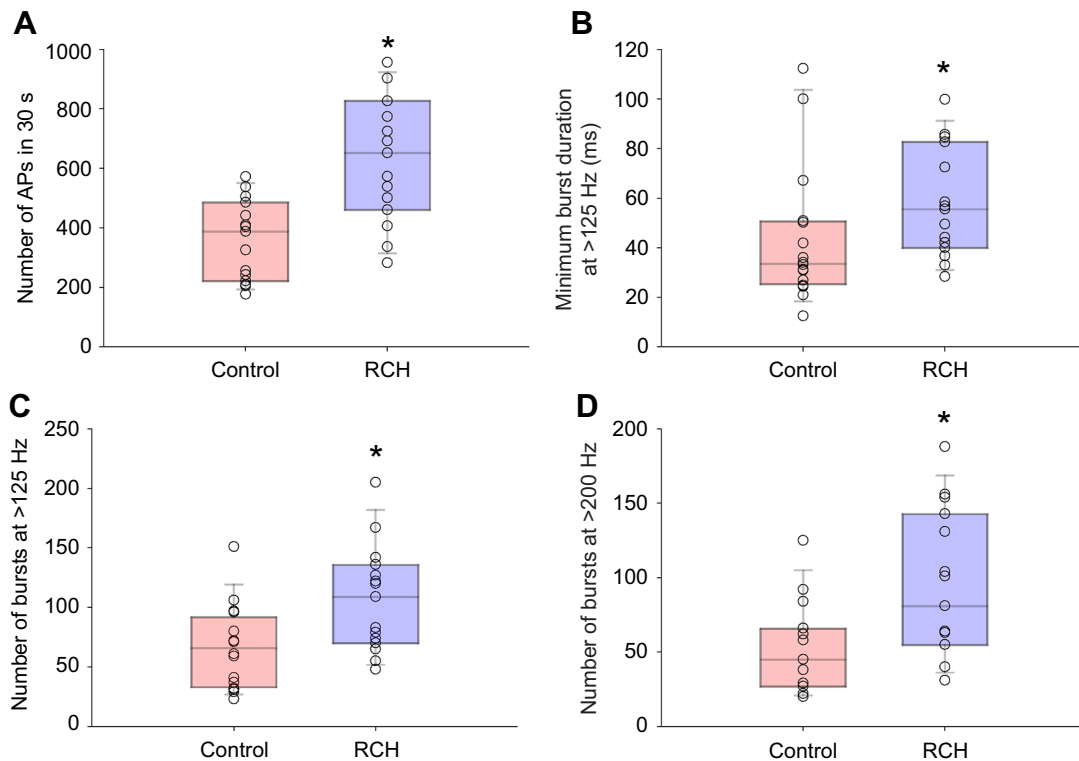


**Fig. 3. RCH increases responsiveness of lobula giant movement detector (LGMD)/DCMD circuit to 30 s of visual stimulation.** (A) Total number of DCMD action potentials (APs). (B) Maximum duration of bursts at frequencies >125 Hz. (C) Number of bursts at frequencies >125 Hz. (D) Number of bursts at frequencies >200 Hz. Box plots indicate median, 25th and 75th percentiles and whiskers to 10th and 90th percentiles overlaid with individual data points. Asterisk indicates *P*<0.05.

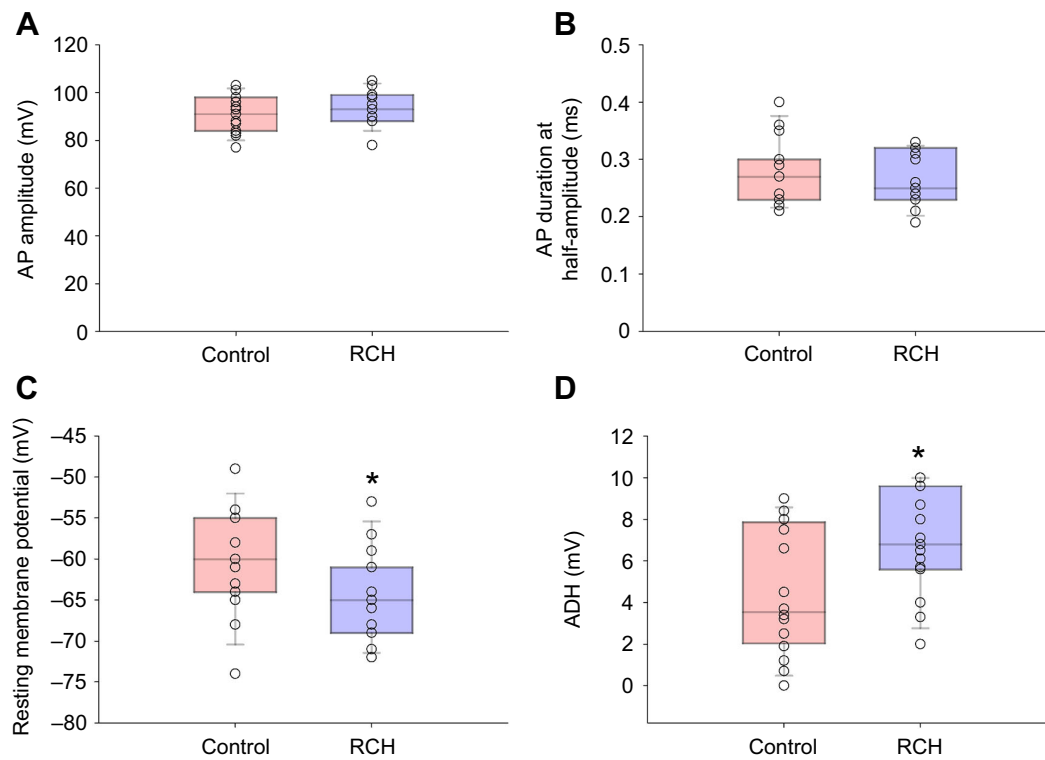


**Fig. 4. RCH affects membrane potential but not action potential parameters.** (A) Action potential amplitude measured from positive peak to negative trough of after-hyperpolarization. (B) Action potential duration measured at half-amplitude. (C) Resting membrane potential. (D) Amplitude of the ADH generated by 1000 action potentials at 100 Hz. Box plots indicate median, 25th and 75th percentiles and whiskers to 10th and 90th percentiles overlaid with individual data points. Asterisk indicates  $P < 0.05$ .

excitability of the visual circuit in the brain that drives DCMD activity. For reasons we discuss below, we suggest that RCH mediates arousal of the visual circuitry via the release of the neurohormone octopamine.

Measurement of NKA activity in tissue homogenates is convenient but sensitive to technical procedures and open to misinterpretation (Moyes et al., 2021). Nevertheless, pretreatments that delay the occurrence of SD and speed recovery do not change the NKA protein level ( $\alpha$  subunit) and have a mild or no effect on its activity in homogenates. Heat shock pretreatment in locusts delays hyperthermic SD and anoxic coma and speeds the recovery from azide-induced SD and  $K^+$ -induced SD with no change in the abundance of the NKA  $\alpha$  subunit and only a mild increase in NKA activity of homogenized nervous tissue (Hou et al., 2014). Cold acclimation in *Drosophila* delays chill coma with no change in the abundance of NKA  $\alpha$  subunits and a decrease in NKA activity of homogenates (Cheslock et al., 2021; MacMillan et al., 2015a). We found that RCH does not change NKA activity in homogenized nervous tissue and extrapolate from that to suggest that overall NKA enzyme abundance in the CNS is not affected by RCH. However, this does not exclude the possibility that NKA activity *in situ* is affected by the treatment, through mechanisms including mass action effects or allosteric regulators.

Our electrophysiological measures of DCMD activity in response to visual and electrical stimulation are determined by the properties of looming-sensitive visual circuitry in the brain (affecting the pattern of firing) and, separately, the properties of the DCMD axon (affecting axonal performance such as frequency-dependent conduction velocity). We found a robust effect of RCH on the excitability of the circuitry in the brain such that 30 s of visual stimulation evoked more action potentials with more

high-frequency bursts, which are required to trigger evasive behaviour. Also, RCH increased the duration of bursts of action potentials at frequencies  $\geq 125$  Hz. Peak firing frequency is an indicator of performance that declines under some stressful conditions (e.g. hypoxia; Money et al., 2014). Although there was no statistical effect of RCH on peak frequency, 5 RCH animals had peak frequencies above 900 Hz whereas only 2 control animals did. We interpret these results as RCH triggering arousal, which reduces habituation of the visual circuitry in *L. migratoria* (Bacon et al., 1995; Rind et al., 2008). This interpretation is supported by the observation that the arousal/dishabituation is evoked by application of octopamine or stimulation of protocerebral octopaminergic neurons (Bacon et al., 1995) and inhibited by the octopamine receptor antagonist epinastine (Rind et al., 2008), and the effects of RCH on chill coma and anoxic coma are similarly mimicked by application of octopamine and inhibited by epinastine (Srithiphaphirom et al., 2019; Srithiphaphirom and Robertson, 2022).

An important consideration is the effect of isolation during the pretreatment. For example, some effects on DCMD activity in isolated food-deprived locusts compared with non-isolated controls have been attributed to the effects of isolation (Cross et al., 2017). In the current investigation, to avoid confounds, both controls and RCH locusts were isolated in the dark for 5 h. A defining characteristic of locusts is that they exist as two separate phenotypes, the gregarious and solitary phases, depending on the level of crowding and contact with conspecifics (Pflüger and Bräunig, 2021). Whereas morphological alterations associated with switching between phases are possible only between moults, behavioural and biochemical changes can arise within hours of isolation or crowding (Anstey et al., 2009; Ma et al., 2015;

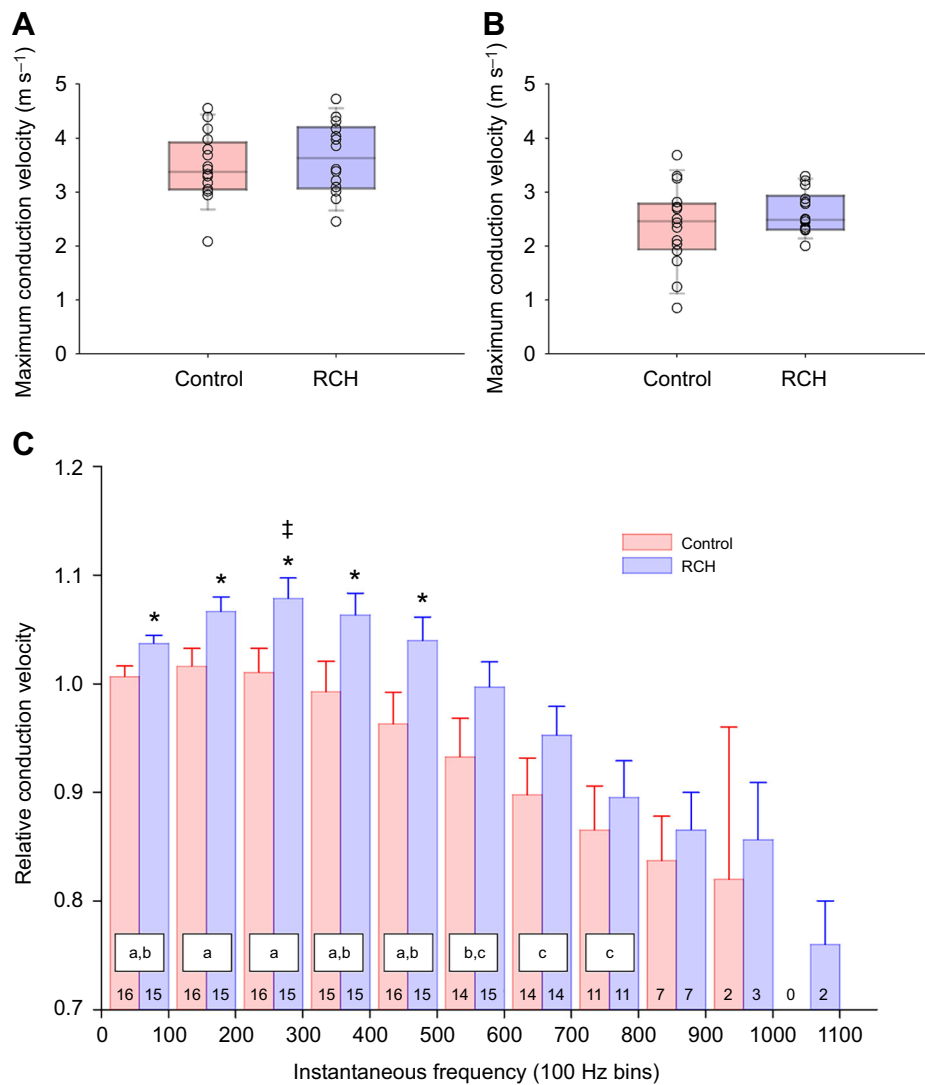


**Fig. 5. RCH has no effect on maximum and minimum conduction velocity but enhances supernormal conduction in the axon.** (A) Maximum conduction velocity. (B) Minimum conduction velocity. In A and B, box plots indicate median, 25th and 75th percentiles and whiskers to 10th and 90th percentiles overlaid with individual data points. (C) Relative conduction velocity binned for different 100 Hz instantaneous frequency ranges. For clarity the columns for control and RCH are illustrated side by side but the frequency ranges are the same for each treatment. Numbers in the columns indicate sample size, tailing off at higher frequencies because not all preparations achieved high-frequency firing. Letters in boxes indicate effects of frequency up to 800 Hz, independent of treatment; different letters indicate  $P < 0.05$  by Holm-Šidák after two-way ANOVA. Asterisks indicate effect of treatment within frequencies determined by one-way ANOVA ( $P < 0.05$ ). Double-dagger indicates peak relative conduction velocity different from low-frequency relative conduction velocity within RCH determined by Student's  $t$ -test ( $P < 0.05$ ).

Rogers et al., 2014; Simpson et al., 2001). Moreover, the DCMD responses of gregarious locusts are more resistant to habituation (Matheson et al., 2004; Rogers et al., 2007, 2010) and the switch to solitary behaviour may be partially dependent on a decrease in octopamine levels (Ma et al., 2015). Hence, an alternative way of interpreting our results is that the isolation of both control and RCH groups induced some behavioural (i.e. CNS) phase change towards the solitary state but this was slower in the RCH group because of the lower temperature. However, this interpretation would imply that RCH had no effect independent of cold-induced slowing of solitarization. Given the volume of data in the literature showing that RCH delays chill coma, which is a failure of ion homeostasis in the nervous system, including in insects that do not exhibit phase polyphenism, we favour the interpretation that RCH had a positive effect to dishabituate the LGMD/DCMD circuit, although we cannot rule out an effect of slower solitarization in our experiments. With respect to determining whether effects of pretreatment in previous RCH studies (Srithiphaphirom et al., 2019; Srithiphaphirom and Robertson, 2022) could be attributed to an enhancement of NKA activity, the pathway to this end is perhaps immaterial.

The performance of action potential conduction in the axon is distinct from the performance of visual circuitry presynaptic to the DCMD, which generates the pattern of firing. We found no effect of

RCH on the amplitude or duration of the intracellularly recorded action potential, indicating that the properties of the voltage-dependent ion channels generating the action potential are not affected by RCH. RCH hyperpolarized the DCMD axon by  $>4$  mV ( $-60.3$  to  $-64.6$  mV) and increased the ADH evoked by 10 s of firing at 100 Hz by  $>50\%$  (4.5 to 6.9 mV). These results are best explained by the electrogenic effect of enhanced NKA activity. A heat shock pretreatment, which causes trafficking of NKA into neuronal plasma membranes and increases NKA activity (Hou et al., 2014), also hyperpolarizes the DCMD axon, particularly at higher temperatures (Money et al., 2005). Moreover, the ADH in the DCMD axon is eradicated by treatment with the NKA inhibitor ouabain (Money et al., 2014). The fact that the size and shape of action potentials did not change during the ADH shows that it was not generated by the opening or closing of ion channels (i.e. background membrane input resistance did not change; see also Money et al., 2014). Conceivably, the ADH could have been generated by a different electrogenic pump. However, given that it is blocked by ouabain and given the extensive literature on NKA-dependent ADH (see citations in the Introduction), we conclude that the ADH is due to NKA and thus that RCH enhances NKA activity in the nervous system.

Axonal performance of the DCMD can be characterized by the ability to maintain high conduction velocities for high-frequency



firing. In our experiments, seven preparations had maximum firing frequencies >900 Hz and two preparations had firing frequencies >1000 Hz. Even at these high frequencies, conduction velocity was reduced by only ~25%, from ~3.5 m s<sup>-1</sup> maximum conduction velocity at low frequencies of firing to ~2.5 m s<sup>-1</sup> minimum conduction velocity at the highest frequencies. RCH had no effect on maximum or minimum conduction velocities but did induce supernormal conduction whereby conduction velocity increased to a peak at 200–300 Hz. Heat shock improves performance of the DCMD axon and induces a prominent DA that shortens the HA and maintains excitability particularly at high temperatures, which hyperpolarize the resting potential (Money et al., 2005). Modelling indicates that the DA is likely generated by a persistent or resurgent Na<sup>+</sup> current, which enhances action potential firing (Meredith and Rennie, 2020), and which counteracts the hyperpolarizing effect of enhanced NKA activity (Cross and Robertson, 2016). Prior anoxic coma (immersion in water for 30 min) eradicates both the ADH (Money et al., 2014) and supernormal conduction in the axon (Cross et al., 2017). Conversely, we found that RCH increases the ADH and promotes supernormal conduction. Moreover, a computational model of a non-myelinated axon (including Hodgkin–Huxley equations, a variety of voltage-dependent ion currents and the NKA pump) demonstrates that supernormal conduction is enhanced with a higher NKA pump current (Zhang et al., 2017). We propose that RCH enhances performance of the DCMD axon by increasing NKA activity and the Na<sup>+</sup> current underlying the DA. With the reasonable assumption that the increased NKA activity is not restricted to the DCMD or to just axons but is a more general neural response, then this explains the effect of RCH to delay SD evoked by chilling or anoxia, and to speed recovery.

Neural information processing is metabolically costly (Attwell and Laughlin, 2001) and it is increasingly evident that neural properties are dynamically regulated to match performance, and thus the energetic costs of high performance, with current or anticipated environmental conditions. Thus, food scarcity or deprivation modulates sensory processing in ways that would conserve energy in mice (Padamsey et al., 2022), electric fish (Sinnott and Markham, 2015) and blowflies (Longden et al., 2014). In locusts, visual processing (e.g. the LGMD/DCMD circuitry) is modified by prior heat shock (Money et al., 2005), prior anoxia (Money et al., 2014), food deprivation (Cross et al., 2017) and, in our current results, prior chilling via RCH. In tadpoles and mice, a pump-mediated ultraslow afterhyperpolarization (equivalent to the ADH described here) acts as a short-term motor memory of locomotor network activity (for review, see Picton et al., 2017b). The strength of this mechanism in tadpoles is modulated by serotonin and nitric oxide (Hachoumi et al., 2022) but the behavioural relevance of such regulation remains unclear. Given that abiotic stress has similar effects on tadpole swimming motor patterns (Robertson et al., 2010; Robertson and Sillar, 2009), one possibility is that, in addition to neuromodulatory pathways reflecting the internal state of the animal, this regulation of NKA in vertebrates occurs in response to the state of the external environment. Our results show that RCH enhances performance of a visual circuit in the brain and of the DCMD axon that conveys the information from the brain to the thoracic ganglia. Neural shutdown via SD induced by abiotic stress in insects is protective by virtue of reducing energy consumption (Campbell et al., 2018, 2019; Robertson et al., 2020). Hence, the potential energetic costs of RCH enhancing NKA and delaying SD are likely offset by the survival advantages conferred by enabling behaviour at lower temperatures.

## Acknowledgements

We thank Sara Dastjerdi and Phinyaphat Srithiphaphrom for performing the NKA assays and Mads Andersen and Yuyang Wang for their comments on a draft of the manuscript.

## Competing interests

The authors declare no competing or financial interests.

## Author contributions

Conceptualization: R.M.R.; Methodology: R.M.R., C.D.M.; Validation: R.M.R., C.D.M.; Formal analysis: R.M.R.; Investigation: R.M.R.; Resources: R.M.R., C.D.M.; Data curation: R.M.R.; Writing - original draft: R.M.R.; Writing - review & editing: R.M.R., C.D.M.; Visualization: R.M.R.; Supervision: R.M.R., C.D.M.; Project administration: R.M.R.; Funding acquisition: R.M.R., C.D.M.

## Funding

This work was funded by Discovery Grants to R.M.R. (RGPIN/04561-2017) and C.D.M. (RGPIN/94551-2017) from the Natural Sciences and Engineering Research Council of Canada.

## Data availability

Data are available from Queen's University Dataverse: <https://doi.org/10.5683/SP3/JUFVA6>.

## References

- Andersen, M. K. and Overgaard, J. (2019). The central nervous system and muscular system play different roles for chill coma onset and recovery in insects. *Comp. Biochem. Physiol. A Mol. Integr. Physiol.* **233**, 10–16. doi:10.1016/j.cbpa.2019.03.015
- Andersen, J. L., Manenti, T., Sørensen, J. G., MacMillan, H. A., Loeschcke, V. and Overgaard, J. (2015). How to assess *Drosophila* cold tolerance: chill coma temperature and lower lethal temperature are the best predictors of cold distribution limits. *Funct. Ecol.* **29**, 55–65. doi:10.1111/1365-2435.12310
- Andersen, M. K., Folkersen, R., MacMillan, H. A. and Overgaard, J. (2017). Cold acclimation improves chill tolerance in the migratory locust through preservation of ion balance and membrane potential. *J. Exp. Biol.* **220**, 487–496. doi:10.1242/jeb.150813
- Andersen, M. K., Jensen, N. J. S., Robertson, R. M. and Overgaard, J. (2018). Central nervous system shutdown underlies acute cold tolerance in tropical and temperate *Drosophila* species. *J. Exp. Biol.* **221**, jeb179598. doi:10.1242/jeb.179598
- Anstey, M. L., Rogers, S. M., Ott, S. R., Burrows, M. and Simpson, S. J. (2009). Serotonin mediates behavioral gregarization underlying swarm formation in desert locusts. *Science* **323**, 627–630. doi:10.1126/science.1165939
- Armstrong, G. A. B., Rodríguez, E. C. and Meldrum Robertson, R. (2012). Cold hardening modulates K<sup>+</sup> homeostasis in the brain of *Drosophila melanogaster* during chill coma. *J. Insect Physiol.* **58**, 1511–1516. doi:10.1016/j.jinsphys.2012.09.006
- Attwell, D. and Laughlin, S. B. (2001). An energy budget for signaling in the grey matter of the brain. *J. Cereb. Blood Flow Metab.* **21**, 1133–1145. doi:10.1097/00004647-200110000-00001
- Bacon, J. P., Thompson, K. S. and Stern, M. (1995). Identified octopaminergic neurons provide an arousal mechanism in the locust brain. *J. Neurophysiol.* **74**, 2739–2743. doi:10.1152/jn.1995.74.6.2739
- Bucher, D. and Goillard, J.-M. (2011). Beyond faithful conduction: short-term dynamics, neuromodulation, and long-term regulation of spike propagation in the axon. *Prog. Neurobiol.* **94**, 307–346. doi:10.1016/j.pneurobio.2011.06.001
- Campbell, J. B., Andersen, M. K., Overgaard, J. and Harrison, J. F. (2018). Paralytic hypo-energetic state facilitates anoxia tolerance despite ionic imbalance in adult *Drosophila melanogaster*. *J. Exp. Biol.* **221**, jeb177147. doi:10.1242/jeb.177147
- Campbell, J. B., Werkhoven, S. and Harrison, J. F. (2019). Metabolomics of anoxia tolerance in *Drosophila melanogaster*: evidence against substrate limitation and for roles of protective metabolites and paralytic hypometabolism. *Am. J. Physiol. Regul. Integr. Comp. Physiol.* **317**, R442–R450. doi:10.1152/ajpregu.00389.2018
- Cheslock, A., Andersen, M. K. and MacMillan, H. A. (2021). Thermal acclimation alters Na<sup>+</sup>/K<sup>+</sup>-ATPase activity in a tissue-specific manner in *Drosophila melanogaster*. *Comp. Biochem. Physiol. A Mol. Integr. Physiol.* **256**, 110934. doi:10.1016/j.cbpa.2021.110934
- Cross, K. P. and Robertson, R. M. (2016). Ionic mechanisms maintaining action potential conduction velocity at high firing frequencies in an unmyelinated axon. *Physiol. Rep.* **4**, e12814. doi:10.14814/phy2.12814
- Cross, K. P., Britton, S., Mangulins, R., Money, T. G. A. and Robertson, R. M. (2017). Food deprivation and prior anoxic coma have opposite effects on the activity of a visual interneuron in the locust. *J. Insect Physiol.* **98**, 336–346. doi:10.1016/j.jinsphys.2017.02.006



- Findsen, A., Andersen, J. L., Calderon, S. and Overgaard, J. (2013). Rapid cold hardening improves recovery of ion homeostasis and chill coma recovery time in the migratory locust, *Locusta migratoria*. *J. Exp. Biol.* **216**, 1630–1637. doi:10.1242/jeb.081141
- Gabbiani, F., Krapp, H. G. and Laurent, G. (1999). Computation of object approach by a wide-field, motion-sensitive neuron. *J. Neurosci.* **19**, 1122–1141. doi:10.1523/JNEUROSCI.19-03-01122.1999
- Gantz, J. D., Spong, K. E., Seroogy, E. A., Robertson, R. M. and Lee, R. E., Jr. (2020). Effects of brief chilling and desiccation on ion homeostasis in the central nervous system of the migratory locust, *Locusta migratoria*. *Comp. Biochem. Physiol. A Mol. Integr. Physiol.* **249**, 110774. doi:10.1016/j.cbpa.2020.110774
- Gerster, U., Stavenga, D. G. and Backhaus, W. (1997). Na<sup>+</sup>/K<sup>+</sup>-pump activity in photoreceptors of the blowfly *Calliphora*: a model analysis based on membrane potential measurements. *J. Comp. Physiol. A Neuroethol. Sens. Neural Behav. Physiol.* **180**, 113–122. doi:10.1007/s003590050032
- Gray, J. R. (2005). Habituated visual neurons in locusts remain sensitive to novel looming objects. *J. Exp. Biol.* **208**, 2515–2532. doi:10.1242/jeb.01640
- Gray, J. R., Lee, J. K. and Robertson, R. M. (2001). Activity of descending contralateral movement detector neurons and collision avoidance behaviour in response to head-on visual stimuli in locusts. *J. Comp. Physiol. A Neuroethol. Sens. Neural Behav. Physiol.* **187**, 115–129. doi:10.1007/s003590100182
- Gray, J. R., Blinow, E. and Robertson, R. M. (2010). A pair of motion-sensitive neurons in the locust encode approaches of a looming object. *J. Comp. Physiol. A Neuroethol. Sens. Neural Behav. Physiol.* **196**, 927–938. doi:10.1007/s00359-010-0576-7
- Hachoumi, L., Rensner, R., Richmond, C., Picton, L., Zhang, H. and Sillar, K. T. (2022). Bimodal modulation of short-term motor memory via dynamic sodium pumps in a vertebrate spinal cord. *Curr. Biol.* **32**, 1038–1048.e2. doi:10.1016/j.cub.2022.01.012
- Hazell, S. P. and Bale, J. S. (2011). Low temperature thresholds: are chill coma and CT(min) synonymous? *J. Insect Physiol.* **57**, 1085–1089. doi:10.1016/j.jinsphys.2011.04.004
- Hopf, H. C., Lowitzsch, K. and Galland, J. (1976). Conduction velocity during the supernormal and late subnormal periods in human nerve fibres. *J. Neurol.* **211**, 293–298. doi:10.1007/BF00313239
- Hou, N., Armstrong, G. A. B., Chakraborty-Chatterjee, M., Sokolowski, M. B. and Robertson, R. M. (2014). Na<sup>+</sup>-K<sup>+</sup>-ATPase trafficking induced by heat shock pretreatment correlates with increased resistance to anoxia in locusts. *J. Neurophysiol.* **112**, 814–823. doi:10.1152/jn.00201.2014
- Jørgensen, L. B., Robertson, R. M. and Overgaard, J. (2020). Neural dysfunction correlates with heat coma and CT(max) in *Drosophila* but does not set the boundaries for heat stress survival. *J. Exp. Biol.* **223**, jeb218750. doi:10.1242/jeb.218750
- Kelty, J. D. and Lee, R. E., Jr. (1999). Induction of rapid cold hardening by cooling at ecologically relevant rates in *Drosophila melanogaster*. *J. Insect Physiol.* **45**, 719–726. doi:10.1016/S0022-1910(99)00040-2
- Kryvenko, V., Vagin, O., Dada, L. A., Sznajder, J. I. and Vadász, I. (2021). Maturation of the Na,K-ATPase in the endoplasmic reticulum in health and disease. *J. Membr. Biol.* **254**, 447–457. doi:10.1007/s00232-021-00184-z
- Kueh, D., Barnett, W. H., Cymbalyuk, G. S. and Calabrese, R. L. (2016). Na<sup>+</sup>/K<sup>+</sup> pump interacts with the h-current to control bursting activity in central pattern generator neurons of leeches. *Life* **5**, e19322. doi:10.7554/eLife.19322
- Lee, R. E., Jr, Chen, C. P. and Denlinger, D. L. (1987). A rapid cold-hardening process in insects. *Science* **238**, 1415–1417. doi:10.1126/science.238.4832.1415
- Longden, K. D., Muzzu, T., Cook, D. J., Schultz, S. R. and Krapp, H. G. (2014). Nutritional state modulates the neural processing of visual motion. *Curr. Biol.* **24**, 890–895. doi:10.1016/j.cub.2014.03.005
- Ma, Z., Guo, X., Lei, H., Li, T., Hao, S. and Kang, L. (2015). Octopamine and tyramine respectively regulate attractive and repulsive behavior in locust phase changes. *Sci. Rep.* **5**, 8036. doi:10.1038/srep08036
- MacMillan, H. A., Andersen, J. L., Davies, S. A. and Overgaard, J. (2015a). The capacity to maintain ion and water homeostasis underlies interspecific variation in *Drosophila* cold tolerance. *Sci. Rep.* **5**, 18607. doi:10.1038/srep18607
- MacMillan, H. A., Ferguson, L. V., Nicolai, A., Donini, A., Staples, J. F. and Sinclair, B. J. (2015b). Parallel ionoregulatory adjustments underlie phenotypic plasticity and evolution of *Drosophila* cold tolerance. *J. Exp. Biol.* **218**, 423–432. doi:10.1242/jeb.115790
- Matheson, T., Rogers, S. M. and Krapp, H. G. (2004). Plasticity in the visual system is correlated with a change in lifestyle of solitary and gregarious locusts. *J. Neurophysiol.* **91**, 1–12. doi:10.1152/jn.00795.2003
- McMillan, G. A. and Gray, J. R. (2015). Burst firing in a motion-sensitive neural pathway correlates with expansion properties of looming objects that evoke avoidance behaviors. *Front. Integr. Neurosci.* **9**, 60. doi:10.3389/fnint.2015.00060
- Meredith, F. L. and Rennie, K. J. (2020). Persistent and resurgent Na<sup>+</sup> currents in vestibular calyx afferents. *J. Neurophysiol.* **124**, 510–524. doi:10.1152/jn.00124.2020
- Money, T. G. A., Anstey, M. L. and Robertson, R. M. (2005). Heat stress-mediated plasticity in a locust looming-sensitive visual interneuron. *J. Neurophysiol.* **93**, 1908–1919. doi:10.1152/jn.00908.2004
- Money, T. G. A., Sproule, M. K. J., Hamour, A. F. and Robertson, R. M. (2014). Reduction in neural performance following recovery from anoxic stress is mimicked by AMPK pathway activation. *PLoS ONE* **9**, e88570. doi:10.1371/journal.pone.0088570
- Money, T. G. A., Sproule, M. K. J., Cross, K. P. and Robertson, R. M. (2016). Octopamine stabilizes conduction reliability of an unmyelinated axon during hypoxic stress. *J. Neurophysiol.* **116**, 949–959. doi:10.1152/jn.00354.2016
- Moyes, C. D., Dastjerdi, S. H. and Robertson, R. M. (2021). Measuring enzyme activities in crude homogenates: Na<sup>+</sup>/K<sup>+</sup>-ATPase as a case study in optimizing assays. *Comp. Biochem. Physiol. B Biochem. Mol. Biol.* **255**, 110577. doi:10.1016/j.cbpb.2021.110577
- Oshea, M., Rowell, C. H. F. and Williams, J. L. (1974). Anatomy of a locust visual interneuron - descending contralateral movement detector. *J. Exp. Biol.* **60**, 1–12. doi:10.1242/jeb.60.1.1
- Overgaard, J. and MacMillan, H. A. (2017). The integrative physiology of insect chill tolerance. *Annu. Rev. Physiol.* **79**, 187–208. doi:10.1146/annurev-physiol-022516-034142
- Padamsey, Z., Katsanevaki, D., Dupuy, N. and Rochefort, N. L. (2022). Neocortex saves energy by reducing coding precision during food scarcity. *Neuron* **110**, 280–296.e10. doi:10.1016/j.neuron.2021.10.024
- Pflüger, H. J. and Bräunig, P. (2021). One hundred years of phase polymorphism research in locusts. *J. Comp. Physiol. A Neuroethol. Sens. Neural Behav. Physiol.* **207**, 321–326. doi:10.1007/s00359-021-01485-3
- Picton, L. D., Nascimento, F., Broadhead, M. J., Sillar, K. T. and Miles, G. B. (2017a). Sodium pumps mediate activity-dependent changes in mammalian motor networks. *J. Neurosci.* **37**, 906–921. doi:10.1523/JNEUROSCI.2005-16.2016
- Picton, L. D., Zhang, H. and Sillar, K. T. (2017b). Sodium pump regulation of locomotor control circuits. *J. Neurophysiol.* **118**, 1070–1081. doi:10.1152/jn.00066.2017
- Pulver, S. R. and Griffith, L. C. (2010). Spike integration and cellular memory in a rhythmic network from Na<sup>+</sup>/K<sup>+</sup> pump current dynamics. *Nat. Neurosci.* **13**, 53–59. doi:10.1038/nn.2444
- Rind, F. C. (1984). A chemical synapse between two motion detecting neurones in the locust brain. *J. Exp. Biol.* **110**, 143–167. doi:10.1242/jeb.110.1.143
- Rind, F. C. and Simmons, P. J. (1992). Orthopteran DCMD neuron: a reevaluation of responses to moving objects. I. Selective responses to approaching objects. *J. Neurophysiol.* **68**, 1654–1666. doi:10.1152/jn.1992.68.5.1654
- Rind, F. C., Santer, R. D. and Wright, G. A. (2008). Arousal facilitates collision avoidance mediated by a looming sensitive visual neuron in a flying locust. *J. Neurophysiol.* **100**, 670–680. doi:10.1152/jn.01055.2007
- Ritchie, J. M. and Straub, R. W. (1957). The hyperpolarization which follows activity in mammalian non-medullated fibres. *J. Physiol.* **136**, 80–97. doi:10.1113/jphysiol.1957.sp005744
- Robertson, R. M. (2004). Thermal stress and neural function: adaptive mechanisms in insect model systems. *J. Thermal Biol.* **29**, 351–358. doi:10.1016/j.jtherbio.2004.08.073
- Robertson, R. M. and Pearson, K. G. (1982). A preparation for the intracellular analysis of neuronal activity during flight in the locust. *J. Comp. Physiol. A* **146**, 311–320. doi:10.1007/BF00612702
- Robertson, R. M. and Sillar, K. T. (2009). The nitric oxide/cGMP pathway tunes the thermosensitivity of swimming motor patterns in xenopus laevis tadpoles. *J. Neurosci.* **29**, 13945–13951. doi:10.1523/JNEUROSCI.3841-09.2009
- Robertson, R. M., Björnfors, E. R. and Sillar, K. T. (2010). Long-lasting effects of chemical hypoxia on spinal cord function in tadpoles. *Neuroreport* **21**, 943–947. doi:10.1097/WNR.0b013e32833e332d
- Robertson, R. M., Spong, K. E. and Sirthaphirom, P. (2017). Chill coma in the locust, *Locusta migratoria*, is initiated by spreading depolarization in the central nervous system. *Sci. Rep.* **7**, 10297. doi:10.1038/s41598-017-10586-6
- Robertson, R. M., Dawson-Scully, K. D. and Andrew, R. D. (2020). Neural shutdown under stress: an evolutionary perspective on spreading depolarization. *J. Neurophysiol.* **123**, 885–895. doi:10.1152/jn.00724.2019
- Rodgers, C. I., Armstrong, G. A. B., Shoemaker, K. L., LaBrie, J. D., Moyes, C. D. and Robertson, R. M. (2007). Stress preconditioning of spreading depression in the locust CNS. *PLoS ONE* **2**, e1366. doi:10.1371/journal.pone.0001366
- Rodgers, C. I., Armstrong, G. A. B. and Robertson, R. M. (2010). Coma in response to environmental stress in the locust: A model for cortical spreading depression. *J. Insect Physiol.* **56**, 980–990. doi:10.1016/j.jinsphys.2010.03.030
- Rogers, S. M., Krapp, H. G., Burrows, M. and Matheson, T. (2007). Compensatory plasticity at an identified synapse tunes a visuomotor pathway. *J. Neurosci.* **27**, 4621–4633. doi:10.1523/JNEUROSCI.4615-06.2007
- Rogers, S. M., Harston, G. W., Kilburn-Toppin, F., Matheson, T., Burrows, M., Gabbiani, F. and Krapp, H. G. (2010). Spatiotemporal receptive field properties of a looming-sensitive neuron in solitary and gregarious phases of the desert locust. *J. Neurophysiol.* **103**, 779–792. doi:10.1152/jn.00855.2009
- Rogers, S. M., Cullen, D. A., Anstey, M. L., Burrows, M., Despland, E., Dodgson, T., Matheson, T., Ott, S. R., Stettin, K., Sword, G. A. et al. (2014). Rapid behavioural gregarization in the desert locust, *Schistocerca gregaria* entails synchronous changes in both activity and attraction to conspecifics. *J. Insect Physiol.* **65**, 9–26. doi:10.1016/j.jinsphys.2014.04.004

- Rowell, C. F.** (1971). The orthopteran descending movement detector (DMD) neurones: a characterisation and review. *Z. Vergl. Physiol.* **73**, 167-194. doi:10.1007/BF00304131
- Santer, R. D., Simmons, P. J., Rind, F. C.** (2005). Gliding behaviour elicited by lateral looming stimuli in flying locusts. *J. Comp. Physiol. A Neuroethol. Sens. Neural Behav. Physiol.* **191**, 61-73. doi:10.1007/s00359-004-0572-x
- Santer, R. D., Rind, F. C., Stafford, R. and Simmons, P. J.** (2006). Role of an identified looming-sensitive neuron in triggering a flying locust's escape. *J. Neurophysiol.* **95**, 3391-3400. doi:10.1152/jn.00024.2006
- Santer, R. D., Yamawaki, Y., Rind, F. C. and Simmons, P. J.** (2008). Preparing for escape: an examination of the role of the DCMD neuron in locust escape jumps. *J. Comp. Physiol. A Neuroethol. Sens. Neural Behav. Physiol.* **194**, 69-77. doi:10.1007/s00359-007-0289-8
- Simmons, P. J., Rind, F. C. and Santer, R. D.** (2010). Escapes with and without preparation: The neuroethology of visual startle in locusts. *J. Insect Physiol.* **56**, 876-883. doi:10.1016/j.jinsphys.2010.04.015
- Simpson, S. J., Despland, E., Hägele, B. F. and Dodgson, T.** (2001). Gregarious behavior in desert locusts is evoked by touching their back legs. *Proc. Natl. Acad. Sci. USA* **98**, 3895-3897. doi:10.1073/pnas.071527998
- Sinnett, P. M. and Markham, M. R.** (2015). Food deprivation reduces and leptin increases the amplitude of an active sensory and communication signal in a weakly electric fish. *Horm. Behav.* **71**, 31-40. doi:10.1016/j.yhbeh.2015.03.010
- Spong, K. E., Andrew, R. D. and Robertson, R. M.** (2016). Mechanisms of spreading depolarization in vertebrate and insect central nervous systems. *J. Neurophysiol.* **116**, 1117-1127. doi:10.1152/jn.00352.2016
- Srithiphaphirom, P. and Robertson, R. M.** (2022). Rapid cold hardening delays the onset of anoxia-induced coma via an octopaminergic pathway in *Locusta migratoria*. *J. Insect Physiol.* **137**, 104360. doi:10.1016/j.jinsphys.2022.104360
- Srithiphaphirom, P., Lavallee, S. and Robertson, R. M.** (2019). Rapid cold hardening and octopamine modulate chill tolerance in *Locusta migratoria*. *Comp. Biochem. Physiol. A Mol. Integr. Physiol.* **234**, 28-35. doi:10.1016/j.cbpa.2019.04.007
- Teets, N. M. and Denlinger, D. L.** (2013). Physiological mechanisms of seasonal and rapid cold-hardening in insects. *Physiol. Entomol.* **38**, 105-116. doi:10.1111/phen.12019
- Teets, N. M., Gantz, J. D. and Kawarasaki, Y.** (2020). Rapid cold hardening: ecological relevance, physiological mechanisms and new perspectives. *J. Exp. Biol.* **223**, jeb203448. doi:10.1242/jeb.203448
- Zhang, H. Y. and Sillar, K. T.** (2012). Short-term memory of motor network performance via activity-dependent potentiation of Na<sup>+</sup>/K<sup>+</sup> pump function. *Curr. Biol.* **22**, 526-531. doi:10.1016/j.cub.2012.01.058
- Zhang, Y., Bucher, D. and Nadim, F.** (2017). Ionic mechanisms underlying history-dependence of conduction delay in an unmyelinated axon. *Elife* **6**, e25382. doi:10.7554/eLife.25382